Corrosive Wear of SiC Whisker- and Particulate-Reinforced 6061 Aluminum Alloy Composites

S.Y. YU, H. ISHII, and T.H. CHUANG

Wear tests on SiC whisker- and SiC particulate-reinforced 6061-T6 aluminum matrix composites (SiCw/Al and SiCp/Al), fabricated using a high pressure infiltration method, were performed in laboratory air, ion-exchanged water and a 3 pct NaCl aqueous solution using a block-on-ring type apparatus. The effects of environment, applied load, and rotational (sliding) speed on the wear properties against a sintered alumina block were evaluated. Electrochemical measurements in ion-exchanged water and a 3 pct NaCl aqueous solution were also made under the same conditions as the wear tests. A comparison was made with the properties of the matrix aluminum alloy 6061-T6. The SiC-reinforced composites exhibited better wear resistance compared with the monolithic 6061 Al alloy even in a 3 pct NaCl aqueous solution. Increase in the wear resistance depended on the shape, size, and volume fraction of the SiC reinforcement. Good correlation was obtained between corrosion resistance and corrosion wear. The ratios of wear volume due to the corrosive effect to noncorrosive wear were 23 to 83 pct, depending on the wear conditions.

I. INTRODUCTION

METAL matrix composites (MMCs) are well-known for their superior mechanical and tribological properties.[1] As for wear of ceramic whisker- or particulate-reinforced aluminum alloy composites, a reasonable amount of data has been published in the literature.[2–14] However, most of the results were obtained in ambient air and little is known about corrosive wear of MMCs.[15] In practical situations, even when it is not always apparent whether corrosive action is involved, there are many cases where corrosion is jointly responsible for wear of metal components, since the corrosion product would be removed continuously by the wearing action. Thus, it is important to know the degree of the corrosive effect on wear, but this is not yet well established. As for the corrosive wear of MMCs, it is expected that their properties may be greatly different from a prediction derived from those of monolithic alloys, since they are made of two constituents, each having a different electrochemical behavior.

The interactive effects of abrasion and corrosion on mild steel plate were studied as a function of abrasive load, corrosion time, and the frequency of abrasive and corrosive treatments by Nöel and Ball.[16] Their results revealed that the initial rate of corrosion was independent of the abrasive load but that the percentage contribution of corrosion to wear decreased with increasing abrasive load. It was also found that when the frequency of exposure to abrasion and corrosion was increased, the wear loss for a constant total amount of abrasion and corrosion increased. The performance of various aluminum alloys in abrasive-corrosive wear conditions which simulate those encountered in mining environments was investigated by Meyer-Rodenbeck *et al.*[17] Their results indicated that pitting corrosion with low volume losses and corrosion rates occurred for the wrought alloys 1200, 3004, 5083, 5251, 6063, 6082, 6261, and 7071, owing to small localized differences in electrode potential at constituent sites. Furthermore, localized attack with accelerated volume losses occurred for the wrought alloys 2014 and 7075 and Al-Si cast alloys. This was due to electrolytic action between phases and microconstituents which were rich in silicon and copper and, therefore, strongly cathodic with respect to aluminum. Wear-corrosion tests of a composite metal (18Cr 9Ni stainless steel) containing WC particles (150 to 190 μm in size) were carried out in a water-sand medium containing various concentrations of sulfuric, hydrochloric, and nitric acids by Ji and Tang.[15] The results showed that the weight loss of specimens which were wear corroded in strong acid-sand media decreased when the compactness (volume percent) of the WC particles in the composite increased, and that the boundaries around WC particles and other carbides in the matrix of materials were preferentially wear corroded in acid-sand media. As mentioned previously, while various interesting results have been obtained for the corrosive wear of various materials, no study has been done so far on the relation between the electrochemical properties and wear resistance.

In the present investigation, wear tests of SiC whisker- and SiC particulate-reinforced 6061 aluminum alloy were performed in laboratory air, ion-exchanged water and a 3 pct NaCl aqueous solution using a block-on-ring type apparatus, and the effects of environment, applied load, and rotational (or sliding) speed of the specimen on the wear properties were evaluated. Furthermore, the relation between corrosion wear properties and corrosion resistance in ion-exchanged water and 3 pct NaCl aqueous solution was examined.

S.Y. YU, Engineer, is with the System-Manufacturing Center, Chung-Shan Institute of Science and Technology, Taipei, Taiwan, 237, Republic of China. H. ISHII, Professor, is with the Department of Mechanical Engineering, Shizuoka University, Hamamatsu, 432, Japan. T.H. CHUANG, Professor, is with the Institute of Materials Science and Engineering, National Taiwan University, Taipei, Taiwan, 106, Republic of China.

Manuscript submitted July 27, 1995.

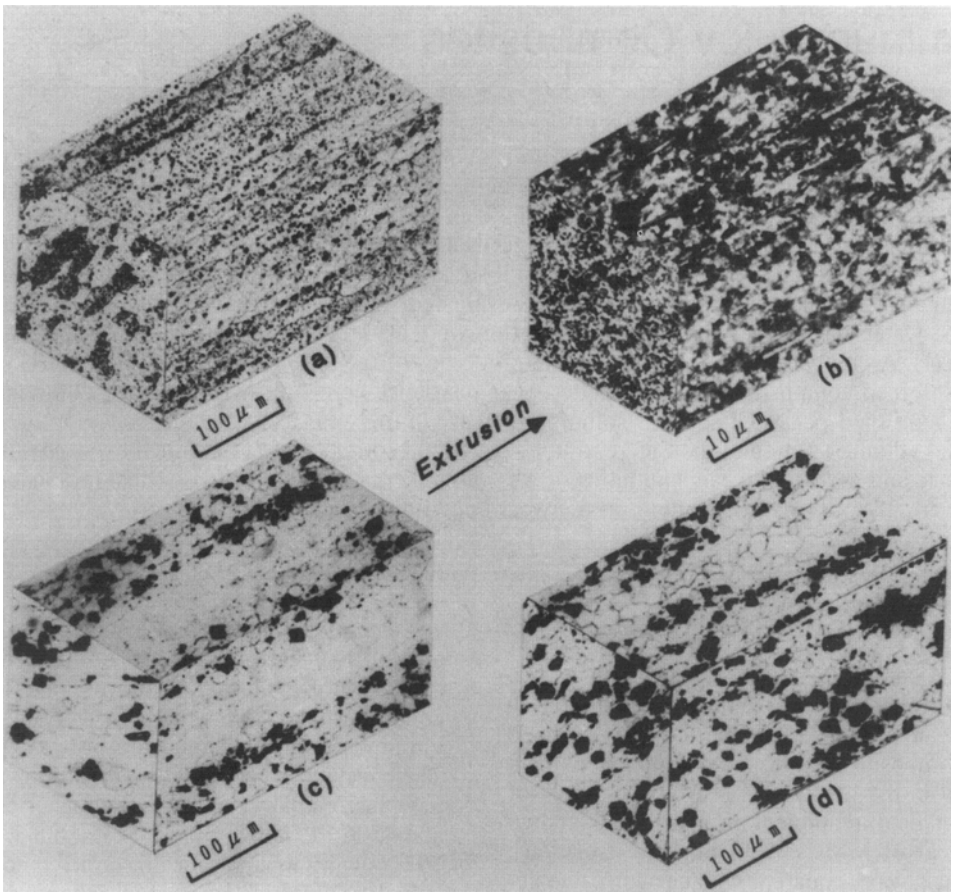

Fig. 1—Three-dimensional micrographs of (*a*) 6061 Al, (*b*) SiCw/Al, (*c*) 5-SiCp/Al, and (*d*) 10-SiCp/Al.

Table I. Mechanical Properties of Materials

Materials	E (GPa)	σ_{UTS} (MPa)	σ_{ys} (MPa)	ε (Pct)	Hv	Density (kg/m³)
6061 Al(L)	67	365	342	11.5	121	2680.4
6061 Al(T)	63	352	326	12.4	125	2680.4
SiCw/Al(L)	117	608	454	2.3	167	2810.3
SiCw/Al(T)	102	418	353	1.8	179	2810.3
5-SiCp/Al(L)	71	371	347	11.2	128	2706.4
5-SiCp/Al(T)	70	347	331	9.5	132	2706.4
10-SiCp/Al(L)	75	378	352	10.7	134	2725.1
10-SiCp/Al(T)	75	354	336	8.6	138	2725.1

II. EXPERIMENTAL PROCEDURE

A. *Materials*

Two types of MMCs used in the present study were SiC whisker- and SiC particulate-reinforced 6061 aluminum alloy composites. In addition to these MMCs, the monolithic 6061 aluminum alloy fabricated using a similar procedure was studied as a reference material. These test materials are simply denoted as SiCw/Al, SiCp/Al, and 6061 Al hereafter in the text.

Billets (200 mm in diameter) fabricated by using a high pressure infiltration method were hot extruded into square bars 52 mm in side length, followed by a T6 treatment. While the volume fraction of the reinforcement in the SiCw/Al was estimated at around 25 pct, two volume fractions of 5 and 10 pct were prepared for the SiCp/Al. They will be denoted as 5-SiCp/Al and 10-SiCp/Al, respectively, whenever the volume fraction is to be specified. The size of the SiC particulates ranged from 6 to 30 μm in diameter. Since extrusion was applied, randomly oriented whiskers were forced to align to the longitudinal (L) direction in the SiCw/Al bar. Their dimensions ranged from 0.5 to 1.0 μm in diameter and about 7 μm in length.

Figure 1 shows typical microstructures of the materials used in the present investigation, and their mechanical properties together with the densities are listed in Table I. The yield strength, tensile strength, and hardness as well as the Young's modulus and the density of the 6061 Al increased, and the ductility decreased, following reinforcement with SiC whiskers or SiC particulates. Especially noted were a prominent strengthening effect and a strong orientation dependency of the mechanical properties following reinforcement with the SiC whiskers. Wear properties were obtained for the L-oriented specimens and also for the T-oriented specimens in the SiCw/Al because of the strong orientation dependency of its tensile properties.

B. *Wear Test*

For wear tests in laboratory air (dry wear at room temperature between 20 °C and 25 °C, with humidity between 70 and 80 pct), ion-exchanged water, and 3 pct NaCl aqueous solution, a block-on-ring apparatus was used. The schematic diagram of the tester with the sliding direction of the SiCw/Al specimens is shown in Figure 2. A block (wear pair) made of sintered 99.5 pct Al_2O_3 (21 × 21 × 21 mm³, Hv 1460 ± 20, and surface roughness of 1.0 μm) was

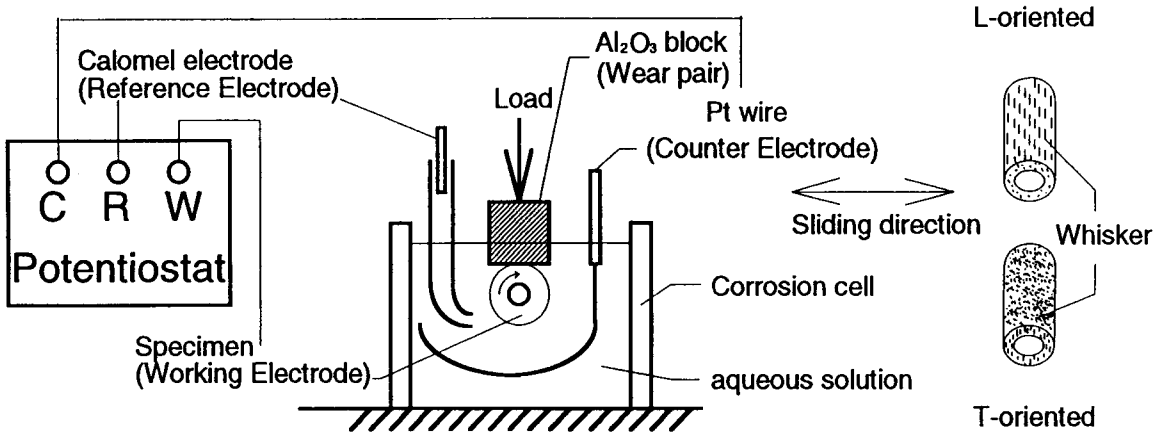

Fig. 2—Schematic diagram of the wear apparatus.

fixed, and a load was applied to a ring specimen. A wear pair of sintered Al_2O_3, insulator was selected to avoid any influence on the electrochemical data of wear specimens. The ring-shaped wear specimens (20, 12.7, and 15 mm in outer diameter, inner diameter, and length, respectively) with a finished surface of arithmetic average roughness 0.5 μm were machined mechanically from the bars. The wear tests were executed at loads of 5, 15, and 25 N for 1 hour at rotational speeds of 100, 300, and 500 rpm. An electronic balance having an accuracy of 0.0001 g was used to measure the weight loss. After testing in 3 pct NaCl aqueous solution, the specimens were polished slightly using cotton, and then cleaned ultrasonically in ion-exchanged water and dried. Wear volume was calculated from the ratio of weight loss to density, and wear rate was computed using the sliding distance and the wear volume. Most of the data for wear tests was taken from the average of three measurements. The standard deviation is about ± 15 pct.

The surfaces of the worn specimens were observed using a scanning electron microscope. Since the hardness of the wear pair (99.5 pct Al_2O_3 ceramic block) was far higher than that of the specimens (aluminum matrix composites) and its wear volume was very small, the wear properties of the wear pair were not studied in the present experiment.

C. *Electrochemical Measurement*

Electrochemical properties in ion-exchanged water and 3 pct NaCl aqueous solution were measured under the same conditions as the wear tests using a Model 363 potentiostat/galvanostat from EG&G Princeton Applied Research (Princeton, NJ). The specimen and a platinum wire which encircled the specimen served as a working electrode and a counterelectrode, respectively. A saturated calomel electrode was used as a reference electrode. The potentiostatic anodic polarization curves were obtained by applying potentials ranging from rest (current near zero) to 1.5 V at intervals of 0.1 V. The open circuit potentials of specimens were measured prior to the polarization test. At each applied potential, the wear lasted 2 to 4 minutes until the corrosion current became stable. The standard deviations for corrosion potential and corrosion current density are about ± 15 mV and ± 4 μA/cm^2, respectively.

III. EXPERIMENTAL RESULTS AND DISCUSSION

A. *The Effect of Applied Load, Rotational Speed, and Environment on the Wear Volume and Wear Rate*

Tables II and III show the wear volume and wear rate under various experimental conditions of applied load, rotational speed, and environment. In order to clarify the effect of these factors on the wear volume and wear rate, graphical representations were made. Figures 3 through 6 show the results. As expected, the wear volume of each material increased linearly with the load and the speed. On the other hand, the wear rate increased linearly with the load but decreased with the speed. As for the environmental effect, the wear volume increased in order of laboratory air, ion-exchanged water, and 3 pct NaCl aqueous solution. Wear volumes in the aqueous solution tests were larger than those of dry wear, because wear debris was carried away by the solution.

Figure 7 shows the worn surfaces of 10-SiCp/Al in three environments at an applied load of 15 N and a rotational speed of 300 rpm. As shown in Figure 7(a), wear debris adhered to the worn surface for the dry wear. In the ion-exchanged water, since the wear debris was carried away, the worn surface was very clean, and plowing can be seen (Figure 7(b)). In the 3 pct NaCl aqueous solution, the corrosive product can be seen in addition to the plowing (Figure 7(c)).

B. *The Effect of SiC Reinforcement on the Wear Resistance*

As was shown in Tables II and III, the wear volume increased in order of 10-SiCp/Al, L-oriented SiCw/Al, T-oriented SiCw/Al, 5-SiCp/Al, and 6061 Al, and the composites exhibited better wear resistance than did 6061 Al in every environment. The SiC reinforcement improved the wear resistance of 6061 Al. Comparing the results of 10-SiCp/Al and 5-SiCp/Al, it is clear that the wear resistance of the MMC increased with the volume fraction of SiC reinforcement. Furthermore, since the SiCw/Al composite with higher volume fraction showed inferior wear resistance compared to 10-SiCp/Al, we can infer that the shape and size of the SiC reinforcement had greater influence on the wear resistance.

Further details can be found in the worn surfaces of the

Table II. Wear Volumes of Materials under Different Conditions (mm³/h)

Wear Conditions		10-SiCp/Al	SiCw/Al(L)	SiCw/Al(T)	5-SiCp/Al	6061 Al
	A	2.16	3.18	3.51	6.09	22.63
5 N, 100 rpm	B	7.62	8.48	8.83	13.99	37.63
	C	13.96	15.29	15.78	21.57	53.39
	A	2.92	4.52	4.73	10.97	29.84
5 N, 300 rpm	B	14.52	23.42	24.83	35.67	61.23
	C	21.79	33.30	34.90	47.04	83.31
	A	3.47	5.44	5.66	16.62	37.16
5 N, 500 rpm	B	25.42	40.35	40.78	48.34	79.84
	C	33.15	43.16	44.12	63.97	108.12
	A	5.43	9.35	10.22	26.08	44.52
15 N, 100 rpm	B	22.74	30.81	32.07	37.27	58.92
	C	38.35	49.65	51.84	61.79	94.35
	A	6.79	12.42	13.43	37.89	70.42
15 N, 300 rpm	B	46.76	63.06	65.95	76.38	129.59
	C	64.19	84.37	88.79	105.86	181.26
	A	8.04	14.95	18.47	51.88	89.43
15 N, 500 rpm	B	70.77	90.95	93.83	117.39	200.90
	C	89.52	114.08	118.64	149.98	263.80
	A	8.90	15.77	16.63	48.99	86.13
25 N, 100 rpm	B	56.98	73.85	75.24	87.55	113.95
	C	76.25	99.29	101.80	123.82	179.95
	A	10.66	19.11	23.59	67.08	115.49
25 N, 300 rpm	B	80.62	104.87	105.22	122.30	202.13
	C	102.74	134.00	135.50	161.94	277.11
	A	13.01	25.64	31.18	85.14	140.04
25 N, 500 rpm	B	116.12	142.05	146.88	181.44	321.96
	C	145.89	174.76	181.90	226.39	404.89

A: dry wear, B: ion-exchanged water, and C: 3 pct NaCl solution.

Table III. Wear Rates of Materials under Different Conditions (mm³/m)

Wear Conditions		10-SiCp/Al	SiCw/Al(L)	SiCw/Al(T)	5-SiCp/Al	6061 Al
	A	5.75×10^{-3}	8.45×10^{-3}	9.30×10^{-3}	1.62×10^{-2}	6.01×10^{-2}
5 N, 100 rpm	B	2.02×10^{-2}	2.25×10^{-2}	2.34×10^{-2}	3.71×10^{-2}	1.00×10^{-1}
	C	3.72×10^{-2}	4.06×10^{-2}	4.18×10^{-2}	5.70×10^{-2}	1.42×10^{-1}
	A	2.58×10^{-3}	4.00×10^{-3}	4.18×10^{-3}	9.70×10^{-3}	2.64×10^{-2}
5 N, 300 rpm	B	1.39×10^{-2}	2.07×10^{-2}	2.19×10^{-2}	3.15×10^{-2}	5.40×10^{-2}
	C	1.93×10^{-2}	2.94×10^{-2}	3.08×10^{-2}	4.16×10^{-2}	7.35×10^{-2}
	A	1.84×10^{-3}	2.88×10^{-3}	3.01×10^{-3}	8.80×10^{-3}	1.97×10^{-2}
5 N, 500 rpm	B	1.35×10^{-2}	2.04×10^{-2}	2.16×10^{-2}	2.56×10^{-2}	4.23×10^{-2}
	C	1.76×10^{-2}	2.29×10^{-2}	2.34×10^{-2}	3.40×10^{-2}	5.75×10^{-2}
	A	1.44×10^{-2}	2.48×10^{-2}	2.72×10^{-2}	6.92×10^{-2}	1.18×10^{-1}
15 N, 100 rpm	B	6.03×10^{-2}	8.18×10^{-2}	8.51×10^{-2}	9.88×10^{-2}	1.56×10^{-1}
	C	1.02×10^{-1}	1.32×10^{-1}	1.38×10^{-1}	1.64×10^{-1}	2.51×10^{-1}
	A	6.00×10^{-3}	1.10×10^{-2}	1.19×10^{-2}	3.34×10^{-2}	6.22×10^{-2}
15 N, 300 rpm	B	4.14×10^{-2}	5.58×10^{-2}	5.84×10^{-2}	6.75×10^{-2}	1.15×10^{-1}
	C	5.67×10^{-2}	7.45×10^{-2}	7.85×10^{-2}	9.35×10^{-2}	1.61×10^{-1}
	A	4.26×10^{-3}	7.94×10^{-3}	9.79×10^{-2}	2.75×10^{-2}	4.74×10^{-2}
15 N, 500 rpm	B	3.75×10^{-2}	4.83×10^{-2}	4.98×10^{-2}	6.22×10^{-2}	1.07×10^{-1}
	C	4.76×10^{-2}	6.04×10^{-2}	6.30×10^{-2}	7.95×10^{-2}	1.40×10^{-1}
	A	2.36×10^{-2}	4.18×10^{-2}	4.40×10^{-2}	1.30×10^{-1}	2.28×10^{-1}
25 N, 100 rpm	B	1.51×10^{-1}	1.96×10^{-1}	1.99×10^{-1}	2.32×10^{-1}	3.03×10^{-1}
	C	2.02×10^{-1}	2.63×10^{-1}	2.70×10^{-1}	3.27×10^{-1}	4.78×10^{-1}
	A	9.42×10^{-3}	1.69×10^{-2}	2.09×10^{-2}	5.93×10^{-2}	1.02×10^{-1}
25 N, 300 rpm	B	7.12×10^{-2}	9.28×10^{-2}	9.30×10^{-2}	1.08×10^{-1}	1.78×10^{-1}
	C	9.08×10^{-2}	1.18×10^{-1}	1.20×10^{-1}	1.43×10^{-1}	2.45×10^{-1}
	A	6.90×10^{-3}	1.36×10^{-2}	1.65×10^{-2}	4.53×10^{-2}	7.42×10^{-2}
25 N, 500 rpm	B	6.15×10^{-2}	7.52×10^{-2}	7.80×10^{-2}	9.62×10^{-2}	1.71×10^{-1}
	C	7.75×10^{-2}	9.28×10^{-2}	9.65×10^{-2}	1.20×10^{-1}	2.14×10^{-1}

A: dry wear, B: ion-exchanged water, and C: 3 pct NaCl solution.

composites. In Figure 8, the worn surfaces and the cross section perpendicular to the worn surfaces of L-oriented SiCw/Al and 5-SiCp/Al in dry wear and in ion-exchanged water at an applied load of 15 N and rotational speed of

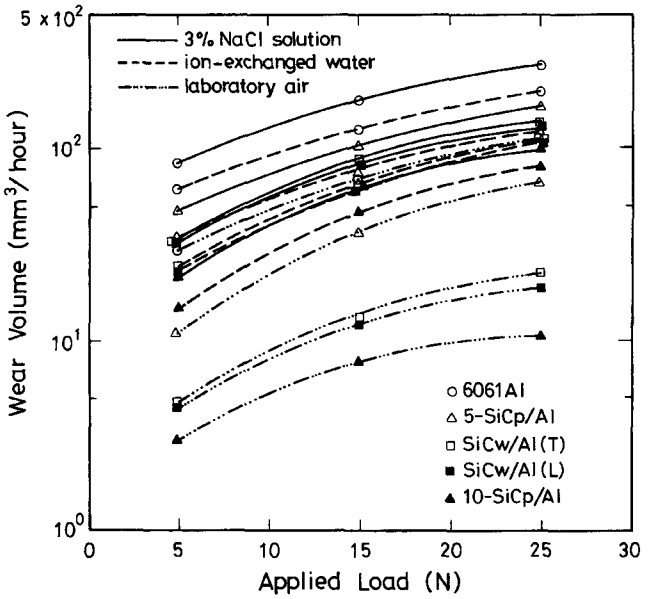

Fig. 3—Effect of the applied load on the wear volumes in three environments. (Rotational speed: 300 rpm.)

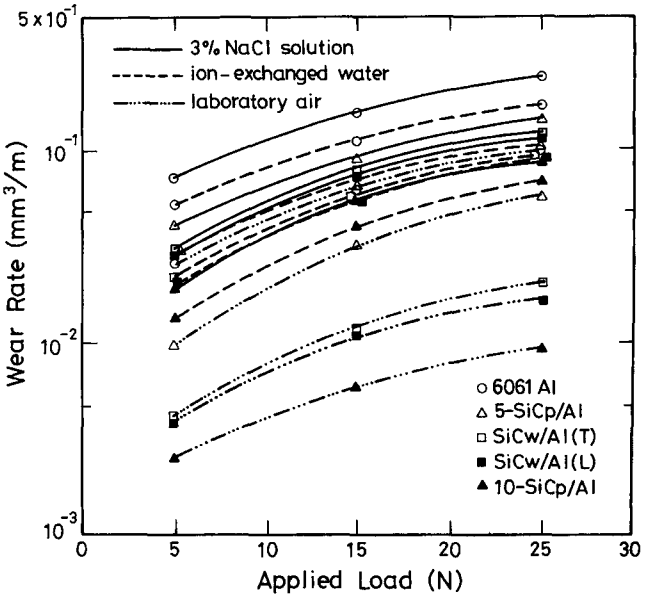

Fig. 5—Effect of the applied load on the wear rates in three environments. (Rotational speed: 300 rpm.)

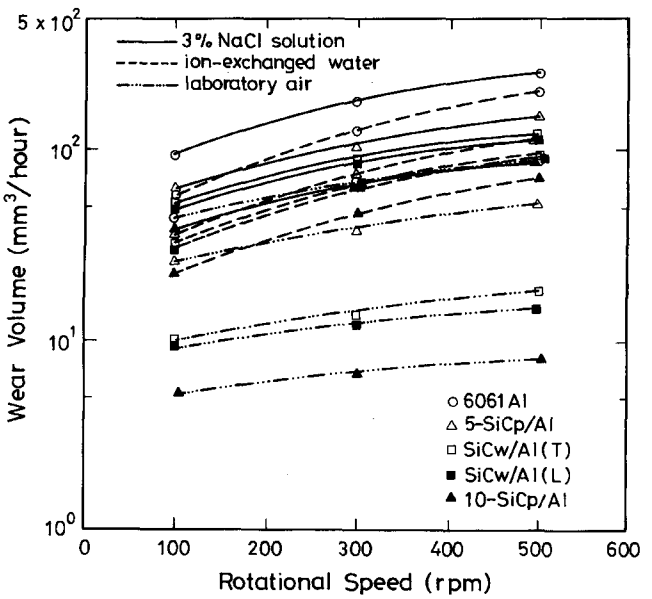

Fig. 4—Effect of the rotational speed on the wear volumes in three environments. (Applied load: 15 N.)

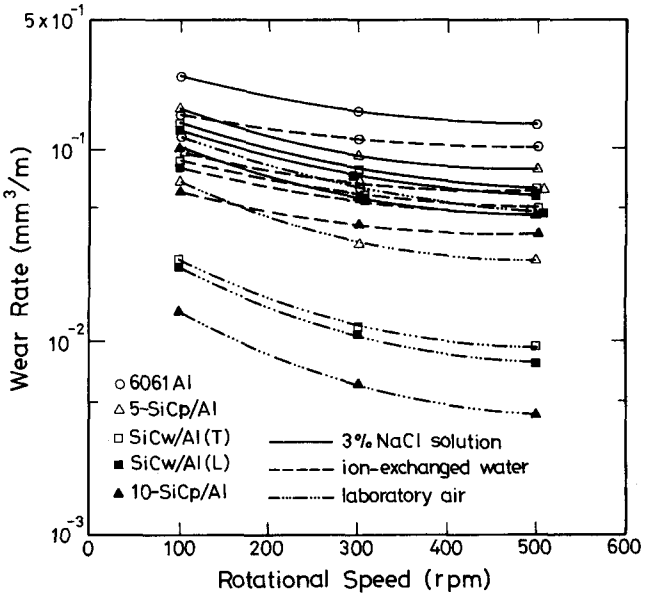

Fig. 6—Effect of the rotational speed on the wear rates in three environments. (Applied load: 15 N.)

300 rpm are shown. The interface of the matrix and SiC whisker was fractured by the high shear stress during the wearing process (Figures 8(a) and (c)), while the SiC particulates were still well protected by the matrix (Figures 8(b) and (d)). This suggests that better wear resistance was obtained in the SiCp specimens than in the SiCw specimens because of the shape and dimensions of the SiC reinforcement. In addition, the wear depth of the aluminum matrix decreased ($\Delta D_2 < \Delta D_1$) with the decrease in interspacing between SiC reinforcements, as shown in Figure 8(d). Since MMCs with a higher volume fraction of SiC reinforcement possess, on average, smaller reinforcement interspacing, their wear depth should also be lower. In short, the wear resistance of the composites depended on the shape, size, and volume fraction of the SiC reinforcement. However, from the results of wear volume and volume fraction in those materials, the shape and size seem to exhibit larger effects than does the volume fraction.

C. *The Relation between Corrosion Wear Properties and Corrosion Resistance*

When tested in aqueous solution, either in ion-exchanged water or in 3 pct NaCl aqueous solution, a hydrated aluminum oxide film formed on the surface which was worn out by the pair, and a fresh abraded active surface was created again. This process was continued by rotation of the specimen. Figures 9 and 10 show the representative effect of the applied load on the corrosion potentials and current densities for T-oriented SiCw/Al in ion-exchanged water and 3 pct NaCl aqueous solution when the rotational speed was 300 rpm. The higher the load, the more fresh

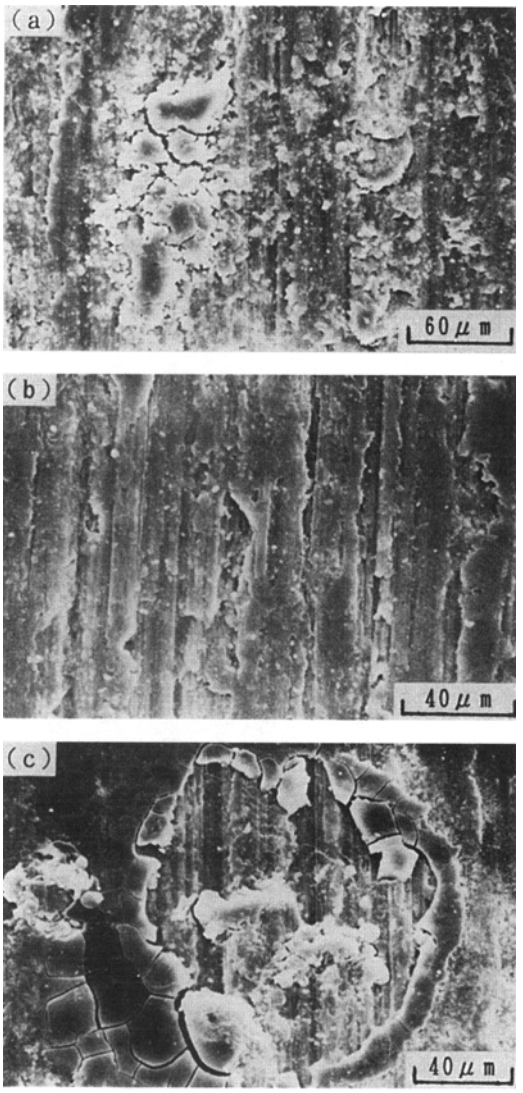

Fig. 7—Surfaces of 10-SiCp/Al tested in (*a*) air, (*b*) ion-exchanged water, and (*c*) 3 pct NaCl aqueous solution. (Applied load: 15 N, rotational speed: 300 rpm.)

abraded area which came into contact with the solution was formed, owing to the larger wear depth. Thus, the corrosion potential and current density shifted to the active side and the current density increased with the applied load. Since the time needed to repair the oxide film was shortened as the speed increased, more fresh abraded areas were created with the increased speed. Therefore, an effect similar to that of the applied load was observed, the corrosion potential and current density shifted to the active side, and the current density increased with the rotational speed. Figures 11 and 12 show the representative effect of the rotational speed on the corrosion potentials and current densities for T-oriented SiCw/Al at an applied load of 15 N in two liquid environments.

To explore the relationship between corrosion resistance and corrosion wear resistance, the potentiostatic anodic polarization curves of the materials in ion-exchanged water and 3 pct NaCl aqueous solution were obtained. Figure 13 shows an example of the result with an applied load of 15 N and a rotational speed of 300 rpm. On the other hand, when the unit wear depth (average wear depth per wear period) was used to evaluate the corrosion wear resistance, the values for 10-SiCp/Al, L-oriented SiCw/Al, T-oriented SiCw/Al, 5-SiCp/Al, and 6061 Al were calculated as 3.8, 5.0, 5.2, 6.2, and 10.7 nm, respectively, in 3 pct NaCl aqueous solution. It is clear that a material with lower unit wear depth exhibits better wear resistance, and the same order as that for the current density was obtained. The relation between the corrosion resistance and the corrosive wear was confirmed in 3 pct NaCl aqueous solution.

In ion-exchanged water, however, the situation was somewhat different. The corrosion potentials and current densities of T- and L-oriented SiCw/Al were among the lowest in spite of their higher unit wear depth (Figures 9 through 12). The volume fraction of SiC reinforcement seemed to affect the corrosion resistance in ion-exchanged water.

It is also shown in Figures 10, 12, and 13 that the current density of each material in ion-exchanged water was two to three orders smaller than that in 3 pct NaCl aqueous solution. It is natural that more severe wear was observed in 3 pct NaCl aqueous solution than in ion-exchanged water.

D. *The Corrosive Effect*

To analyze the corrosion effect, the corrosion tendencies of the materials under unloaded conditions were sought. Figure 14 shows the representative variation in static corrosion potential with time under unloaded conditions in ion-exchanged water and 3 pct NaCl aqueous solution. It is obvious that the corrosion potentials in ion-exchanged water and in 3 pct NaCl aqueous solution showed opposite tendencies. That is, the corrosion potential changed toward the noble side in ion-exchanged water while it changed toward the active side in 3 pct NaCl aqueous solution.

When an as-polished monolithic aluminum alloy or aluminum matrix composite was immersed in ion-exchanged water, a hydrated aluminum oxide film ($Al_2O_3 \cdot xH_2O$) formed rapidly on aluminum.[18] The corrosion potential thus quickly changed toward the noble side and gradually approached an equilibrium. On the other hand, in 3 pct NaCl aqueous solution, chloride anions took part in the corrosion, causing the break down of the hydrated aluminum oxide. The exposed fresh aluminum alloy exhibited a change of corrosion potential toward the active side.

Furthermore, it appears that the corrosion potential shifted to the noble side with an increasing volume fraction of SiC reinforcement in ion-exchanged water. This result agrees with the corrosion potential and current density shown during the wear test in exchanged water described in Section C. It is known that the existence of SiC reinforcement in MMCs causes the active elements, such as Mg in the aluminum matrix, to diffuse and segregate to the SiC/Al interface.[19] This might explain why the corrosion potential of MMCs became more noble than that of monolithic 6061 aluminum alloy. However, the interfacial products at the SiC/Al interface were more easily destroyed by chloride anions in 3 pct NaCl aqueous solution. This resulted in a tendency for SiC-reinforced composites to become more active than the monolithic 6061 aluminum alloy, which is also shown in Figure 14.

The curves of the corrosion potential with time under unloaded conditions indicate that the corrosion tendency in

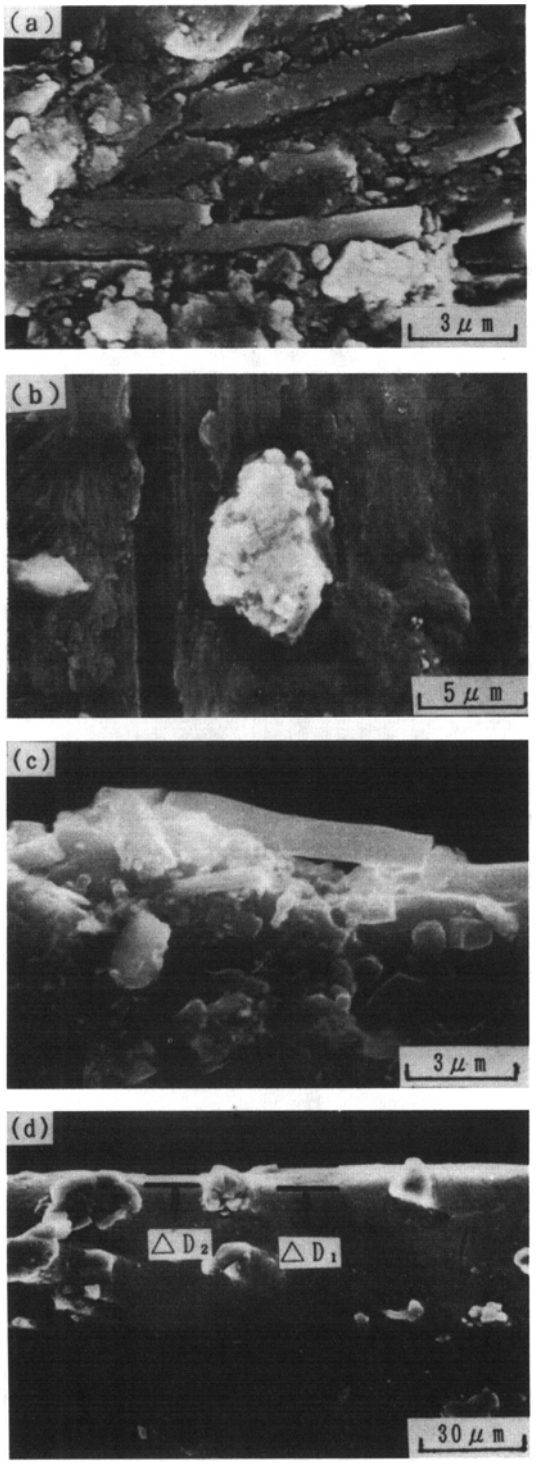

Fig. 8—Surfaces of (*a*) SiCw/Al(L) and (*b*) 5-SiCp/Al tested in air and cross sections of (*c*) SiCw/Al(L) and (*d*) 5-SiCp/Al tested in ion-exchanged water. (Applied load: 15 N, rotational speed: 300 rpm.)

3 pct NaCl aqueous solution was much higher than that in ion-exchanged water. Furthermore, as mentioned previously, the corrosion rate (current density) in ion-exchanged water was two to three orders smaller than that in 3 pct NaCl aqueous solution, wear debris was carried away by the solution, and corrosive product was not observed. Therefore, the wear in ion-exchanged water and in 3 pct NaCl aqueous solution can be regarded as noncorrosive and

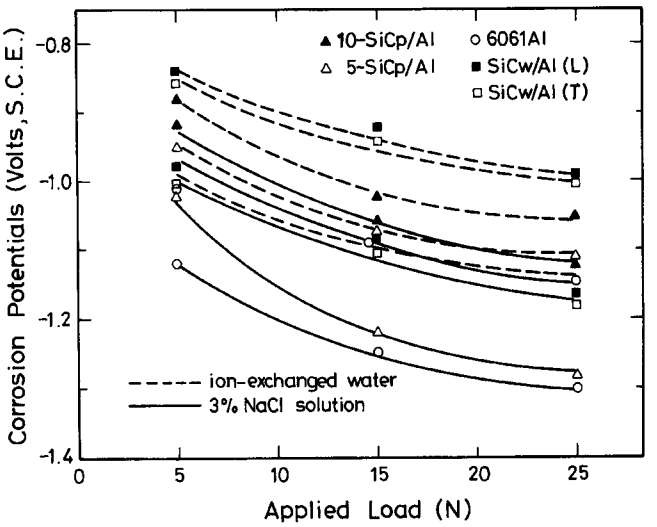

Fig. 9—Effect of the applied load on the corrosion potentials. (Rotational speed: 300 rpm.)

corrosive, respectively. Based on this conclusion, the difference in the wear volume between the tests in the two environments of ion-exchanged water and 3 pct NaCl aqueous solution was considered as the corrosive effect caused by 3 pct NaCl aqueous solution, and the values are shown in Table IV. In Table V, the ratios of these values to the wear volumes in ion-exchanged water under different conditions of loads and rotational speeds are listed. The ratio decreased with an increase in the applied load and rotational speed, and approached approximately the same value at a higher rotational speed (500 rpm). The ratio of wear volume due to the corrosive effect to that in noncorrosive wear ranged from 0.23 to 0.83, depending on the wear conditions. Furthermore, the corrosive wear volumes of those materials were also proportional to their electrochemical properties.

Pitting, as shown in Figure 15, was observed on the worn surface only after the potentiostatic anodic polarization test in 3 pct NaCl aqueous solution, and no pitting was observed under the other wearing conditions. This might have occurred because the growth rate of pit was accelerated by the applied potential in 3 pct NaCl aqueous solution and exceeded the unit wear depth. Pitting occurred at the interface between the matrix and the Mg_2Si precipitates[20] for SiCp/Al and 6061 Al (Figure 16(a)) and at the interface of the whisker and the matrix for SiCw/Al (Figure 16(b)).

IV. CONCLUSIONS

The wear behavior of SiC whisker- and SiC particulate-reinforced 6061-T6 aluminum alloy was obtained in three environments of laboratory air, ion-exchanged water, and 3 pct NaCl aqueous solution, and the results were compared with those of the monolithic alloy.

1. The 6061 Al composites reinforced with SiC whiskers or particulates exhibited excellent wear resistance compared with the monolithic alloy even in 3 pct NaCl aqueous solution. The increase in the wear resistance depended on the shape, size, and volume fraction of the SiC reinforcement. The wear resistance increased in the

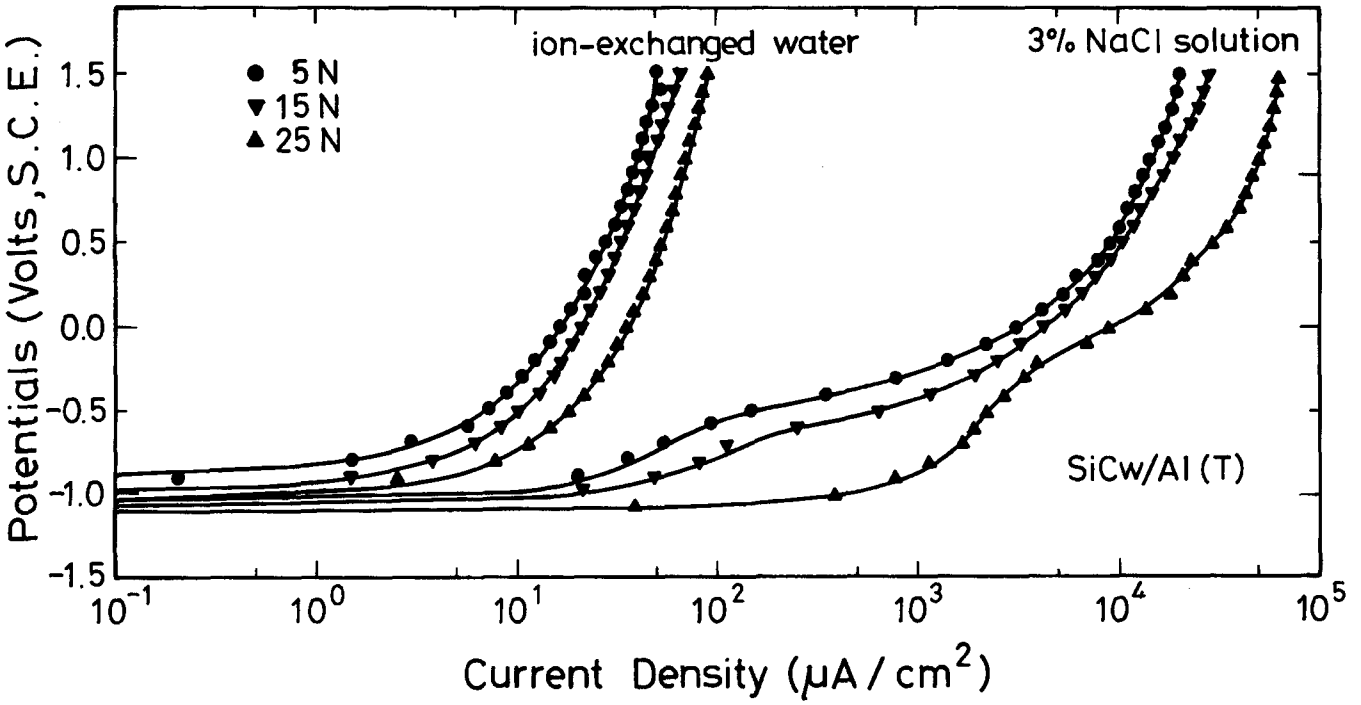

Fig. 10—Effect of the applied load on the potentiostatic anodic polarization curves of SiCw/Al(T). (Rotational speed: 300 rpm.)

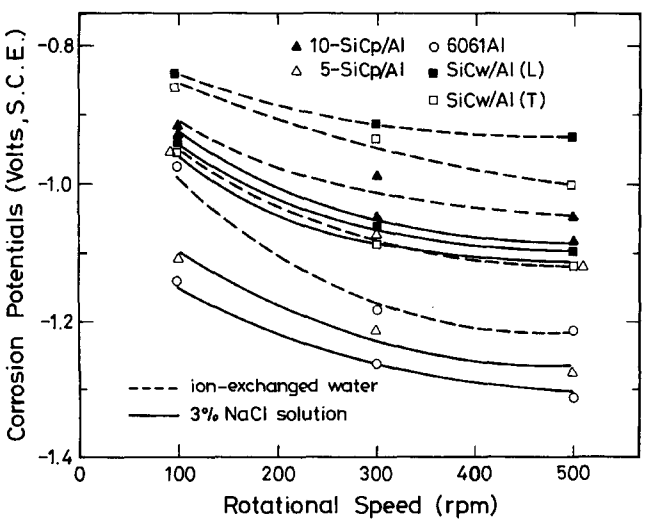

Fig. 11—Effect of the rotational speed on the corrosion potentials. (Applied load: 15 N.)

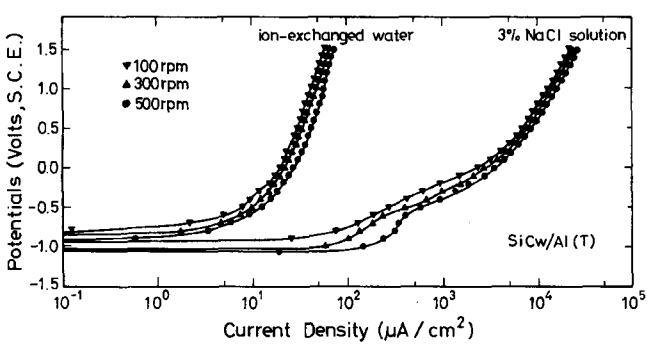

Fig. 12—Effect of the rotational speed on the potentiostatic anodic polarization curves of SiCw/Al(T). (Applied load: 15 N.)

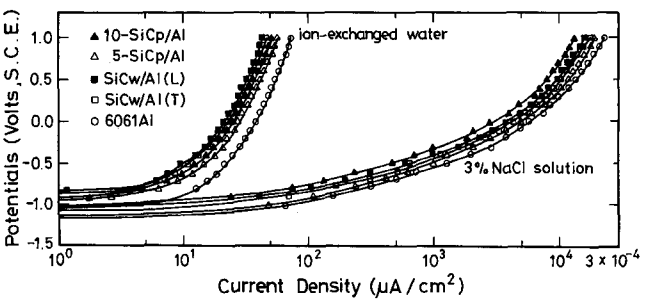

Fig. 13—Potentiostatic anodic polarization curves. (Applied load: 5 N, rotational speed: 300 rpm.)

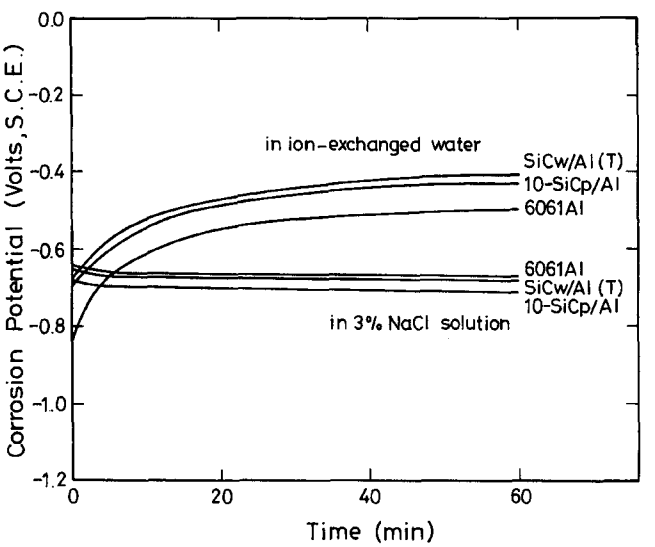

Fig. 14—Relation between the corrosion potential and exposed time (unloaded).

Table IV. Wear Volumes Caused by the Corrosive Effect (mm^3/h)

Wear Conditions	10-SiCp/Al	SiCw/Al(L)	SiCw/Al(T)	5-SiCp/Al	6061 Al
5 N, 100 rpm	6.34	6.81	6.95	7.58	15.76
5 N, 300 rpm	7.27	9.88	10.07	11.37	22.08
5 N, 500 rpm	7.73	12.51	13.34	15.63	28.28
15 N, 100 rpm	15.61	18.47	19.77	24.52	35.43
15 N, 300 rpm	17.43	21.31	22.84	29.30	51.67
15 N, 500 rpm	18.75	23.13	24.81	32.59	62.90
25 N, 100 rpm	19.27	25.44	26.56	36.27	65.80
25 N, 300 rpm	22.12	29.13	30.28	39.64	74.98
25 N, 500 rpm	25.77	32.71	35.02	44.95	82.52

Table V. Ratio of Wear Volume Due to the Corrosive Effect to that in Noncorrosive Wear

Wear Conditions	10-SiCp/Al	SiCw/Al(L)	SiCw/Al(T)	5-SiCp/Al	6061 Al
5 N, 100 rpm	0.83	0.80	0.79	0.54	0.42
5 N, 300 rpm	0.50	0.42	0.41	0.32	0.36
5 N, 500 rpm	0.30	0.31	0.33	0.32	0.35
15 N, 100 rpm	0.69	0.60	0.62	0.66	0.60
15 N, 300 rpm	0.37	0.34	0.35	0.38	0.40
15 N, 500 rpm	0.26	0.25	0.26	0.28	0.31
25 N, 100 rpm	0.34	0.34	0.35	0.41	0.49
25 N, 300 rpm	0.27	0.28	0.29	0.32	0.37
25 N, 500 rpm	0.26	0.23	0.24	0.25	0.26

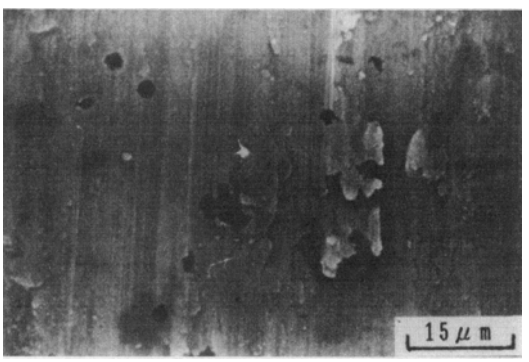

Fig. 15—The surface of 6061 Al in 3 pct NaCl solution after the polarization test. (Applied load: 15 N, rotational speed: 300 rpm.)

order of 6061 Al, 5-SiCp/Al, T-oriented SiCw/Al, L-oriented SiCw/Al, and 10-SiCp/Al.

2. The wear volume of the composites and the monolithic alloy increased with an increased applied load and rotational speed of the wear pair.
3. The wear rate of the composites and the monolithic alloy increased with an increased applied load, but it decreased with the increased rotational speed of the wear pair.
4. Good correlation was obtained between the corrosion resistance and the corrosive wear.
5. The ratio of wear volume due to the corrosive effect to that in noncorrosive wear ranged from 0.23 to 0.83, depending on the conditions.
6. Resistance of the composites to both static and wearing corrosion in ion-exchanged water was related directly to the volume fraction of SiC reinforcement.

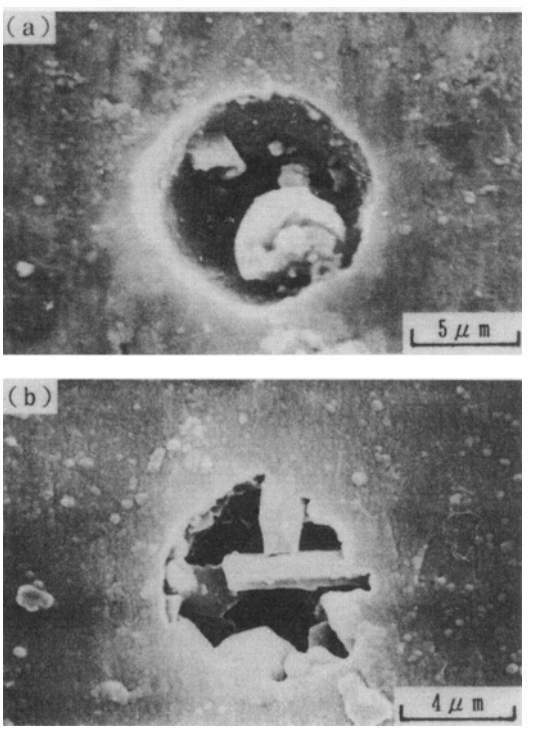

Fig. 16—Nucleation sites of pits in (*a*) 6061 Al and (*b*) SiCw/Al(L) after the polarization test.

REFERENCES

1. P.K. Rohatgi, Y. Liu, and S. Ray: in *Friction, Lubrication, and Wear Technology*, ASM Handbook, The Materials Information Society, Metals Park, OH, 1992, vol. 18, pp. 801-811.
2. S.J. Lin and K.S. Liu: *Wear*, 1988, vol. 121, pp. 1-14.

3. Z. Ma, J. Bi, Y. Lu, H. Shen, and Y. Gao: *Wear*, 1991, vol. 148, pp. 287-93.
4. H.L. Lee, W.H. Lu, and S.L.I. Chan: *Wear*, 1992, vol. 159, pp. 223-31.
5. H.L. Lee, W.H. Lu, and S.L.I. Chan: *Mater. Lett.*, 1992, vol. 15, pp. 49-52.
6. F. Rana and D.M. Stefanescu: *Metall. Trans. A*, 1989, vol. 20A, pp. 1564-66.
7. L. Cao, Y. Wang, and C.K. Yao: *Wear*, 1990, vol. 140, pp. 273-77.
8. A. Wang and H.J. Rack: *Mater. Sci. Eng.*, 1991, vol. A147, pp. 211-14.
9. A. Wang and H.J. Rack: *Wear*, 1991, vol. 147, pp. 355-74.
10. A.T. Alpas and J. Zhang: *Wear*, 1992, vol. 155, pp. 83-104.
11. Y.M. Pan, M.E. Fine, and H.S. Cheng: *Tribol. Trans.*, 1992, vol. 35, pp. 482-90.
12. B.N. Pramila Bai, B.S. Ramasesh, and M.K. Surappa: *Wear*, 1992, vol. 157, pp. 295-304.
13. M. Roy, B. Venkataraman, V.V. Bhanuprasad, Y.R. Mahajan, and G. Sundararajan: *Metall. Trans. A*, 1992, vol. 23A, pp. 2833-47.
14. J. Zhang and A.T. Alpas: *Mater. Sci. Eng.*, 1993, vol. A161, pp. 273-84.
15. J.L. Ji and J.L. Tang: *Wear*, 1990, vol. 138, pp. 23-32.
16. R.E.J. Nöel and A. Ball: *Wear*, 1983, vol. 87, pp. 351-61.
17. G. Meyer-Rodenbeck, T. Hurd, and A. Ball: *Wear*, 1992, vol. 154, pp. 305-17.
18. H.P. Godard, W.B. Jepson, M.R. Bothwell, and R.L. Kane: in *The Corrosion of Light Metals*, Electrochemical Society, Inc., New York, NY, 1967, pp. 3-11.
19. K.S. Foo, W.M. Banks, A.J. Craven, and A. Hendry: *Composites*, 1994, vol. 25 (7), pp. 677-83.
20. I. Dutta and D.L. Bourell: *Mater. Sci. Eng.*, 1989, vol. A112, pp. 67-77.